Inorg. Chem. **2005**, *44*, 6558–6566

Mono-, Di-, and Trinuclear Luminescent Silver(I) and Gold(I) N-Heterocyclic Carbene Complexes Derived from the Picolyl-Substituted Methylimidazolium Salt: 1-Methyl-3-(2-pyridinylmethyl)-1H-imidazolium Tetrafluoroborate

Vincent J. Catalano* and Adam L. Moore

Department of Chemistry, University of Nevada, Reno, Nevada 89557

Received April 19, 2005

The N-heterocyclic carbene (NHC) precursor, 1-methyl-3-(2-pyridinylmethyl)-1H–imidazolium tetrafluoroborate, $[HCH_3im(CH_2py)]BF_4$, reacted with $AgBF_4$ in the presence of aqueous NaOH to produce the silver complex $[Ag(CH_3im(CH_2py))_2]BF_4$ (**1**) which was then reacted with Au(tht)Cl to form the corresponding gold(I) complex, $[Au(CH_3im(CH_2py))_2]BF_4$ (**2**). Complex **2** reacted with 1 equiv of $AgBF_4$ to produce the mixed-metal species $[AuAg(CH_3im(CH_2py))_2](BF_4)_2$ (**3**). The reaction of **2** with 1 equiv of Au(tht)Cl followed by metathesis with $NaBF_4$ produces the dimetallic gold complex $[Au_2(CH_3im(CH_2py))_2](BF_4)_2$ (**4**). The reaction of $[Ag(CH_3im(CH_2py))_2]BF_4$ (**1**) with 1 equiv of $AgBF_4$ produces the trinuclear $[Ag_3(CH_3im(CH_2py))_3(NCCH_3)_2](BF_4)_3$ (**5**) complex, which appears to dissociate into a dimetallic complex in solution. Complexes **1**–**5** were characterized by ^1H NMR, ^{13}C NMR, UV-vis, luminescence spectroscopy, elemental analysis, mass spectrometry, and X-ray crystallography. The $CH_3im(CH_2py)$ ligands in **3** are arranged in a head-to-head fashion spanning a Au–Ag separation of 3.0318(5) Å with the carbene portion of the ligand remaining coordinated to the Au(I) center. In **4**, the ligands are arranged in a head-to-tail fashion with an Au–Au separation of 3.1730(5) Å. In **5**, the ligands bridge the nearly symmetrical Ag_3 triangular core with short Ag–Ag separations of 2.7765(8), 2.7832(8), and 2.7598(8) Å. All of these complexes, including the ligand precursor, are intensely luminescent in solution and the solid state.

Introduction

The attractive interactions between closed-shell metal ions continue to attract attention because of their unexpected bonding and photophysical properties.[1,2] Among the most widely studied are those between d^{10} metals with the most pronounced effects, termed *aurophilicity*, found in the chemistry of gold(I).[3,4] The origin of aurophilic attractions is attributed to correlation effects that are reinforced by relativistic effects.[5] The incorporation of a dissimilar d^{10} metal, like silver(I), produces a dipole moment that can reinforce the $d^{10}-d^{10}$ metal−metal interaction, and often, shorter intermetallic separations are observed within these heterometallic systems.[6]

As part of our continuing study[7,8,9] on the bonding and optical properties of closed-shell heterometallic interactions, we have recently focused our attention on using the now ubiquitous imidazolium-based N-heterocyclic carbene (NHC) ligands[10,11,12] as supports for maintaining mixed-metal as-

* To whom correspondence should be addressed. E-mail: vjc@unr.edu.

(1) Bardají, M.; Laguna, A. *Eur. J. Inorg. Chem.* **2003**, 3069.
(2) Fernández, E. J.; López-de-Luzuriaga, J. M.; Monge, M.; Olmos, M. E.; Pérez, J.; Laguna, A.; Mohamed, A. A.; Fackler, J. P., Jr. *J. Am. Chem. Soc.* **2003**, 125, 2022. (b) Fernández, E. J.; Laguna, A.; López-de-Luzuriaga, J. M.; Mendizabal, F.; Monge, M.; Olmos, M. E.; Pérez, J. *Chem.—Eur. J.* **2003**, *9*, 456. (c) Fernández, E. J.; Laguna, A.; López-de-Luzuriaga, J. M.; Olmos, M. E.; Pérez, J. *Chem. Commun.* **2003**, 1760.
(3) Schmidbaur, H.; Cronje, S.; Djordjevic, B.; Schuster, O. *Chem. Phys.* **2005** *311*, 151.
(4) Schmidbaur, H. *Gold. Bull.* **2000**, *33*, 3.
(5) Pyykkö, P. *Angew. Chem., Int. Ed.* **2004**, *43*, 4412.
(6) Rawashdeh-Omary, M. A.; Omary, M. A.; Fackler, J. P., Jr. *Inorg. Chim. Acta* **2002**, *334*, 376. (b) Fernández, E. J.; Laguna, A.; López-de-Luzuriaga, J. M.; Monge, M.; Pyykkö, P.; Runeberg, N. *Eur. J. Inorg. Chem.* **2002**, 750. (c) Usón, R.; Laguna, A.; Laguna, M.; Usón, A.; Jones, P. G.; Erdbrügger, C. F. *Organometallics* **1987**, *6*, 1778. (d) Usón, R.; Laguna, A.; Laguna, M.; Manzano, B.; Jones, P. G.; Sheldrick, G. M. *J. Chem. Soc., Dalton Trans.* **1984**, 285.
(7) Catalano, V. J.; Malwitz, M. A. *J. Am. Chem. Soc.* **2004**, *126*, 6560.
(8) Catalano, V. J.; Malwitz, M. A. *Inorg. Chem.* **2003**, *42*, 5483.
(9) Catalano, V. J.; Bennett, B. L.; Malwitz, M. A, Yson, R. L.; Kar, H. M.; Muratidis, S.; Horner, S. J. *Comments Inorg. Chem.* **2003**, *24*, 39.
(10) Herrmann, W. A.; Weskamp, T.; Böhm, V. P. W. *Adv. Organomet. Chem.* **2001**, *48*, 1.

10.1021/ic050604+ CCC: $30.25
Published on Web 08/20/2005

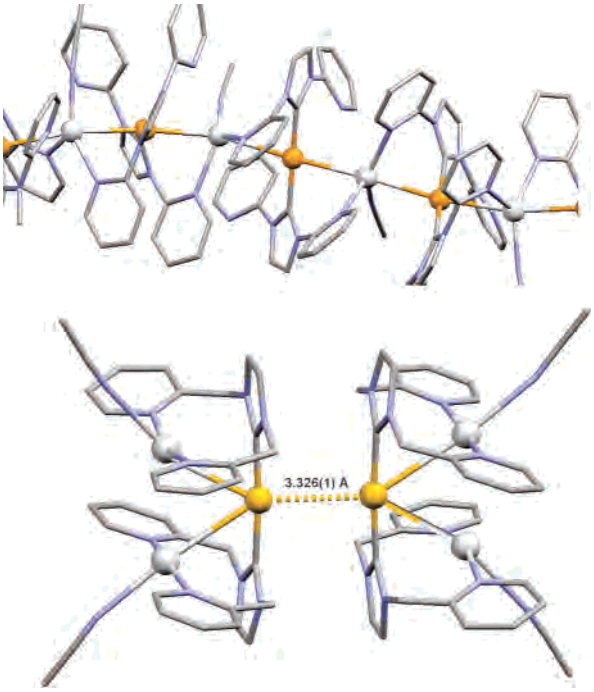

Figure 1. X-ray structural drawing of the cationic portion of helical mixed-metal polymers $\{[AuAg((py)_2im)_2(NCCH_3)]^{2+}\}_n$ (top) and $[AuAg_2((pyCH_2)_2im)_2(NCCH_3)_2](BF_4)_3$ (bottom) with nitrogen atoms shown in blue, carbon atoms in gray, gold atoms in orange, and silver atoms in silver.

Chart 1. Pyridyl- and Picolyl-Substituted NHC Ligands

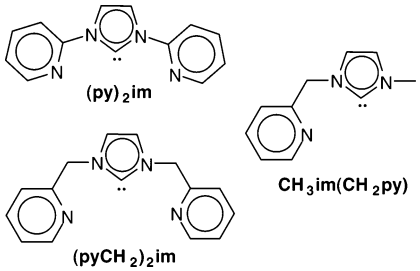

semblies. Recently, we reported[13] a helical mixed-metal coordination polymer (Figure 1, top) with very short Au(I)−Ag(I) separations of 2.8359(4) and 2.9042(2) Å formed by the simple addition of $AgBF_4$ to the homoleptic dipyridyl-substituted (Chart 1) NHC complex, $[Au((py)_2im)_2]BF_4$. This colorless material is highly luminescent in the solid state but readily dissociates into its monomeric components in solution. The origin of this dissociation likely resides in the rigidity imposed by the six-membered dimetallacycle which destabilizes the complex by preventing the close approach of the coordinated pyridyl moiety to the Ag(I) center. Incorporating a methylene spacer between the imidazole ring and the pyridyl moiety alleviates this strain, but no polymer formation was observed. Instead the trimetallic species, $[AuAg_2((pyCH_2)_2im)_2(NCCH_3)_2](BF_4)_3$, containing two silver ions each coordinated to the pyridyl moieties of one carbene ligand and to an acetonitrile molecule in a T-shaped fashion, is produced (Figure 1, bottom). The Au(I)−Ag(I) contacts at 3.220(2) and 3.282(2) Å are considerably longer in this complex than those in the aforementioned $\{[AuAg((py)_2im)_2(NCCH_3)]^{2+}\}_n$ polymer. In the solid state, each trimetallic complex associates with another through a weak (3.326(1) Å) aurophilic attraction.

Herein, we report the Au(I) and Ag(I) chemistry of the related, yet asymmetrical, $CH_3im(CH_2py)$ NHC ligand (Chart 1). It was anticipated that the lack of dual pyridyl donor groups in this ligand would preclude the formation of a trimetallic species while the single picolyl group would promote a less-strained metallacycle which would then lead to a less-labile coordination polymer.

Experimental Section

Solvents were used as received without purification or drying. The preparation of the imidazolium salt, $[H(pyCH_2)_2im]BF_4$, was modified from a published procedure.[14] The preparation of Au(tht)Cl was described elsewhere.[15] UV−vis spectra were obtained using a Hewlett-Packard 8453 diode array spectrometer (1 cm path-length cells). Emission data were recorded using a Spex Fluoromax steady-state fluorimeter. Mass spectral data were acquired using a Waters Micromass ZQ mass spectometer (+ mode, ESI source). Elemental analyses were performed by Desert Analytics in Tuscan, AZ.

Preparation of 1-Methyl-3-(2-pyridinylmethyl)-1H-imidazolium Tetrafluoroborate, $[HCH_3im(CH_2py)]BF_4$. A 50 mL round-bottom flask was charged with 2.000 g (11.7 mmol) of picolyl chloride hydrochloride, 1.788 g (12.9 mmol) of K_2CO_3, and 25 mL of acetone. The mixture was refluxed for 30 min. After which, 0.938 mL of 1-methylimidazole (11.7 mmol) was added, followed by the addition of 1.291 g (11.7 mmol) of $NaBF_4$, and the mixture was further refluxed for 3 days. After the mixture was cooled, it was filtered through Celite. The bright red filtrate was reduced to a minimum volume under vacuum, and a red oil was precipitated with Et_2O. This oil was dissolved in 20 mL of dichloromethane and washed with three 15 mL portions of Et_2O. The solution was reduced to a minimum volume and precipitated with MeOH/EtOH yielding 2.165 g (8.264 mmol) of $[H(Me)(pyCH_2)im](BF_4)$ as a light brown powder (70.2%). ^{1}H NMR (300 MHz, CD_3CN, 25 °C): δ 8.64 (s, 1H), 8.40 (d, 1H), 7.82 (m, 1H), 7.44−7.33 (m, 4H), 5.41 (s, 2H), 3.85 (s, 3H). $^{13}C\{^1H\}$ NMR (75 MHz, CD_3CN, 25 °C): δ 154.25, 151.17, 138.79, 138.09, 125.12, 124.92, 124.32, 124.11, 55.14, 37.22. UV−vis (CH_3CN) λ_{max} (ϵ): 259 (2700), 254 nm (2600).

Preparation of $[Ag(CH_3im(CH_2py))_2]BF_4$ (1). A 50 mL round-bottom flask was charged with 0.500 g (1.91 mmol) of $[HCH_3im(CH_2py)]BF_4$, 25 mL of CH_2Cl_2, 0.185 g (0.954 mmol) of $AgBF_4$, and a catalytic amount of Bu_4NBF_4. The mixture was protected from light and stirred for 10 min; then, NaOH (1 N, 3 mL) was added, and the mixture was stirred for 1 h. The mixture was filtered through Celite, and the clear filtrate was reduced to a minimum volume under vacuum. Complex **1** was precipitated as a white powder (0.838 g, 1.55 mmol, 81.1%) by slow addition of Et_2O. ^{1}H NMR (300 MHz, CD_3CN, 25 °C): δ 8.47 (d, 1H), 7.72 (m, 1H), 7.27−7.16 (m, 4H), 5.36 (s, 2H), 3.78 (s, 3H). $^{13}C\{^1H\}$ NMR (75 MHz, CD_3CN, 25 °C): δ 183.35, 157.53, 151.21, 138.88, 124.82, 124.30, 123.85, 57.88, 39.65. ESI-MS: *m/z* 455 (M+). UV−vis (CH_3CN) λ_{max} (ϵ): 228 nm (13400). Anal. Calcd for $C_{20}H_{22}N_6AgBF_4$: C, 44.39; H, 4.10; N, 15.53. Found: C, 44.30; H, 4.08; N, 15.52.

(11) Lin, I. J. B.; Vasam, C. S. *Comments Inorg. Chem.* **2004**, *25*, 75.
(12) Bourissou, D.; Guerret, O.; Gabbaï, F. P.; Bertrand, G. *Chem. Rev.* **2000**, *100*, 39.
(13) Catalano, V. J.; Malwitz, M. A.; Etogo, A. O. *Inorg. Chem.* **2004**, *43*, 5714.
(14) McGuinness, D. S.; Cavell, K. J. *Organometallics* **2000**, *19*, 741.
(15) Usón, R.; Laguna, A.; Laguna, M. *Inorg. Synth.* **1989**, *26*, 85.

Preparation of $[Au(CH_3im(CH_2py))_2]BF_4$ (2). A 50 mL round-bottom flask was charged with 0.200 g (0.369 mmol) of **1** and 20 mL of CH_2Cl_2. Au(tht)Cl (0.118 g (0.369 mmol)) in 10 mL of CH_2Cl_2 was then added dropwise. The mixture was protected from light and stirred for 15 min, during which a precipitate formed. The solution was filtered through Celite to remove the precipitated AgCl. The clear filtrate was then reduced in volume under vacuum, and a white powder was precipitated using Et_2O yielding 0.180 g (0.286 mmol) of **2** as a white powder (80.7%). ^1H NMR (300 MHz, CD_3CN, 25 °C): δ 8.47 (d, 1H), 7.69 (m, 1H), 7.27−7.18 (m, 4H), 5.44 (s, 2H), 3.80 (s, 3H). $^{13}C\{^1H\}$ NMR (75 MHz, CD_3CN, 25 °C): δ 186.04, 156.92, 150.83, 138.44, 124.47, 124.17, 123.71, 56.87, 38.70. ESI-MS: *m*/*z* 543 (M+). UV−vis(CH_3CN) λ_{max} (ϵ): 261 (15800), 246 (14000), 235 nm (12700). Anal. Calcd for $C_{20}H_{22}N_6AuBF_4$: C, 38.12; H, 3.52; N, 13.33. Found: C, 38.28; H, 3.40; N, 13.34.

Preparation of $[AuAg(CH_3im(CH_2py))_2](BF_4)_2$ (3). A 50 mL round-bottom flask was charged with 0.400 g (0.635 mmol) of **2** and 20 mL of CH_3CN. $AgBF_4$ (0.123 g, 0.635 mmol) in 10 mL of CH_3CN was added dropwise, and the clear mixture was protected from light and stirred for 15 min. The mixture was concentrated under vacuum, and complex **3** (0.501 g (0.608 mmol)) was precipitated from the solution by the slow addition of Et_2O as a fluffy white powder (87.4%). ^1H NMR (300 MHz, CD_3CN, 25 °C): δ 8.54 (d, 1H), 7.89 (dt, 1H), 7.45 (d, 2H), 7.39 (dt, 1H), 7.26 (d, 2H), 5.49 (s, 2H), 3.82 (s, 3H). $^{13}C\{^1H\}$ NMR (75 MHz, CD_3CN, 25 °C): δ 184.97, 157.22, 151.98, 139.60, 125.54, 125.41, 124.79, 124.11, 57.85, 39.28. ESI-MS: *m*/*z* 325.5 (M2+). UV−vis (CH_3CN) λ_{max} (ϵ): 261 (8400), 246 nm (7200). Anal. Calcd for $C_{20}H_{22}N_6AgAuB_2F_8$: C, 29.12; H, 2.69; N, 10.19. Found: C, 29.40; H, 2.69; N, 10.05.

Preparation of $[Au_2(CH_3im(CH_2py))_2](BF_4)_2$ (4). A 50 mL round-bottom flask was charged with 0.100 g (0.184 mmol) of **2**, 20 mL of CH_2Cl_2, and 0.021 g (0.201 mmol) of $NaBF_4$. Au(tht)Cl (0.059 g, 0.184 mmol) was dissolved in 10 mL of CH_2Cl_2 and added dropwise to the solution containing **2**. The clear mixture was protected from light and stirred for 10 min. The addition of Et_2O to the mixture precipitated a white solid which was collected and washed with Et_2O yielding 0.082 g (0.089 mmol) of **4** as a fluffy white powder (56.6%). This material slowly decomposes upon prolonged exposure to UV light and moderate temperature. ^1H NMR (300 MHz, CD_3CN, 25 °C): δ 8.70 (d, 1H), 8.28 (dt, 1H), 8.00 (d, 2H), 7.76 (dt, 1H), 7.29 (s, 2H), 5.81 (bs, 2H), 3.80 (s, 3H). $^{13}C\{^1H\}$NMR (75 MHz, CD_3CN, 25 °C): δ 166.53, 156.56, 154.63, 144.16, 130.08, 128.28, 126.24, 123.51, 57.96, 39.82. ESI-MS: *m*/*z* 740 (M+). UV−vis (CH_3CN) λ_{max} (ϵ): 222 (16300), 245 nm (13800).

Preparation of $[Ag_3(CH_3im(CH_2py))_3(NCCH_3)_2](BF_4)_3$ (5). A 50 mL round-bottom flask was charged with 0.117 g (0.216 mmol) of **1** in 20 mL of CH_2Cl_2. $AgBF_4$ (0.042 g, 0.216 mmol) in 10 mL of CH_3CN was added dropwise. The colorless mixture was protected from light and stirred for 10 min. The mixture was concentrated under vacuum. Precipitation with Et_2O yielded 0.139 g (0.189 mmol) of **5** as a fluffy white powder (87.4%). ^1H NMR (300 MHz, CD_3CN, 25 °C): δ 8.26 (d, 1H), 7.95 (dt, 1H), 7.64 (d, 2H), 7.42 (dt, 1H), 7.35 (d, 2H), 5.46 (s, 2H), 3.76 (s, 3H). $^{13}C\{^1H\}$ NMR (75 MHz, CD_3CN, 25 °C): δ 177.63, 155.56, 152.35, 140.65, 126.21, 125.93, 125.81, 123.88, 57.80, 39.42. ESI-MS: *m*/*z* 1013 (M+). UV−vis (CH_3CN) λ_{max} (ϵ): 254 (5000), 259 nm (4800). IR: ν_{CN} 2324, 2353 cm^{-1}. Anal. Calcd for $C_{30}H_{33}N_9Ag_3B_2F_8$: C, 33.58; H, 3.17; N, 12.24. Found: C, 33.33; H, 3.00; N, 11.31.

X-ray Crystallography. For all complexes, X-ray quality crystals were obtained by slow diffusion of diethyl ether through an ethanol interface into acetonitrile solutions of the complexes. Suitable crystals were coated in a hydrocarbon oil and mounted on a glass fiber. X-ray crystallographic data were collected at low temperature (100 K) using a Bruker SMART Apex CCD diffractometer with Mo Kα radiation and a detector-to-crystal distance of 4.94 cm. Data were collected in a full sphere using four set of frames with 0.3° scans in ω and an exposure time of 10s per frame. The 2θ range extended from 3.0 to 64°. Data were corrected for Lorentz and polarization effects using the SAINT program and corrected for absorption using SADABS or TWINABS. Unit cells were indexed using up to 9999 reflections harvested from the data collection. The structures were solved by direct methods and refined using the SHELXTL 5.12 software package.[16] The crystals of **5** were split, and the data were satisfactorily modeled as a two-component twinned structure (51% and 49%).

Results

The NHC precursor, $[HCH_3im(CH_2py)]^+$, and its silver complex were prepared analogously to the method of McGuinness and Cavell[14] who first prepared the iodide salts of these materials. As depicted in Scheme 1, the homoleptic silver complex, $[Ag(CH_3im(CH_2py))_2]BF_4$ (**1**), cleanly reacts with Au(tht)Cl (tht is tetrahydrothiophene) in a silver carbene transfer reaction to form the corresponding gold(I) complex, $[Au(CH_3im(CH_2py))_2]BF_4$ (**2**). Complex **2** reacts with 1 equiv of $AgBF_4$ to produce the mixed-metal species $[AuAg(CH_3im(CH_2py))_2](BF_4)_2$ (**3**), where the Au(I) center remains bound to the carbene portion of the ligand and the Ag(I) ion coordinates to the two dangling pyridyl groups. Alternatively, the reaction of **2** with 1 equiv of Au(tht)Cl, followed by metathesis with $NaBF_4$, produces the dimetallic gold complex $[Au_2(CH_3im(CH_2py))_2](BF_4)_2$ (**4**), and unlike complex **3**, the two NHC ligands in **4** are bound in a head-to-tail fashion. This material is slightly thermal and photosensitive, and the solid samples of complex **4** slowly decompose upon prolonged exposure to fluorescent room light and room temperature. The reaction of $[Ag(CH_3im(CH_2py))_2]BF_4$ (**1**) with another equivalent of $AgBF_4$ does not exclusively produce the anticipated dimetallic silver complex analogous to **4**. Instead, trinuclear $[Ag_3(CH_3im(CH_2py))_3(NCCH_3)_2](BF_4)_3$ (**5**) is isolated as a solid. At first glance, this species appears to be C_3 symmetric, but its coordination mode is somewhat unusual (vide infra) with a nearly triangular Ag_3 core bridged by the three carbene moieties with each Ag(I) ion coordinated to a pyridyl group. Additionally, two Ag centers are each further coordinated to an acetonitrile molecule. In solution, this species is dynamic and dissociates, presumably, into the corresponding dimetallic $[Ag_2(CH_3im(CH_2py))_3(NCCH_3)_2]^{2+}$ complex from which crystals of **5** are reproducibly isolated.

The carbene precursor and the metal complexes were studied by ^1H NMR spectroscopy, and their spectra are consistent with their proposed formulation. The CD_3CN ^1H NMR spectrum of $[HCH_3im(CH_2py)]BF_4$ exhibits nine proton resonances with the most downfield resonance (8.64 ppm) assigned to the acidic proton at position 1 of the imidazolium ring. The methylene and methyl resonances

(16) *XRD Single-Crystal Software*; Bruker Analytical X-ray Systems: Madison WI, 1999.

Scheme 1

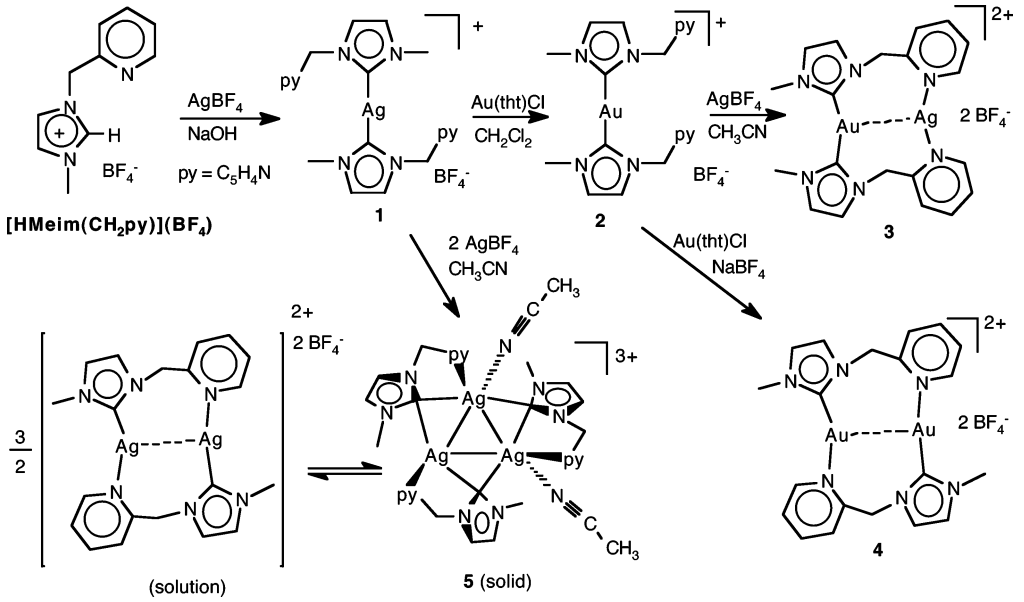

appear at 5.43 and 3.86 ppm, respectively. The reaction with Ag(I) to form the bis-carbene complex, $[Ag(CH_3im(CH_2py))_2]BF_4$ (**1**), causes the most downfield resonance to disappear and minimally shifts the methylene and methyl resonances upfield to 5.36 and 3.78 ppm, respectively. The conversion of this material to $[Au(CH_3im(CH_2py))_2]BF_4$ (**2**) shifts these two resonances back downfield to 5.41 and 3.80 ppm. The addition of $AgBF_4$ to produce the heterodimetallic complex, $[AuAg(CH_3im(CH_2py))_2](BF_4)_2$ (**3**), shifts the methyl resonance to 3.82 ppm. At room temperature, the methylene resonance of **3** appears as a singlet at 5.49 ppm; however, when the temperature was lowered to −90 °C, this signal resolves into an AB quartet centered at 6.02 ppm (δ_A = 6.19, δ_B = 5.84 ppm, $^2J(H_AH_B)$ = 5.4 Hz) (see Supporting Information). From the coalescence point observed at −74 °C, an activation free energy of 8.4 kcal mol^{-1} is calculated.

Likewise, the homodimetallic complex, $[Au_2(CH_3im(CH_2py))_2](BF_4)_2$ (**4**), exhibits a similar dynamic behavior, except that the process is much less facile in this complex. At 25 °C (CD_3CN), no methylene signal is discernible from the baseline while the methyl signal appears as a singlet at 3.80 ppm. Lowering the temperature to −40 °C stops the dynamic process, and an AB quartet centered at 5.81 ppm with δ_A = 6.17, δ_B = 5.43 ppm, and $^2J(H_AH_B)$ = 9 Hz appears (Supporting Information). Heating the sample to near boiling (70 °C) almost produces the fast-exchange limit with a singlet at 5.82 ppm. On the basis of a coalescence temperature of 18.0 °C, a simple analysis of this process yields a $\Delta G^{\ddagger}$ = 10.7 kcal mol^{-1}. The difference in dynamic behavior between **3** and **4** likely stems from the head-to-head versus head-to-tail coordination modes of the ligands.

The ^{1}H NMR spectrum (CD_3CN) of $[Ag_3(CH_3im(CH_2py))_3(NCCH_3)_2](BF_4)_3$ (**5**) appears dynamic and more closely resembles that of **4** with a single methyl resonance at 3.76 ppm and a single nondiastereotopic resonance for the methylene protons at 5.46 ppm. Likewise, the pattern of the pyridyl proton resonances is almost identical to that found in **4** suggesting that the NHC ligand remains coordinated in a similar head-to-tail fashion, consistent with a dimetallic species, rather than the asymmetric trimer observed in the crystal structure. Lowering the temperature to −40 °C did not produce the anticipated stopped-exchange spectrum; instead, it only precipitated the material out of solution. The solubility of the complex in noncoordinating solvents, such as CD_2Cl_2 or $CDCl_3$, is too low for a ^{1}H NMR signal to be detected.

The formulation of $[Ag_2(CH_3im(CH_2py))_2](BF_4)_2$ in solution is further supported by the mass spectrum of **5** whose most intense signal is centered around 734 amu, consistent with the dimetallic formulation, along with much less intense peaks, corresponding to the addition of one and two acetonitrile molecules. A very small peak corresponding to $[Ag_3(CH_3im(CH_2py))_3(CH_3CN)_2](BF_4)^+$ is also observed at 1013 amu.

Complexes **1**−**5** were additionally characterized by X-ray crystallography. Crystallographic information is provided in Table 1. $[Ag(CH_3im(CH_2py))_2]BF_4$ (**1**) crystallizes in the monoclinic space group $P2_1/n$ with one cation and one tetrafluoroborate anion occupying the asymmetric unit. A drawing of the cation is provided in Figure 2, while selected bond distances and angles are presented in Table 2. The cation contains a nearly linearly coordinated Ag(I) ion with a C(1)−Ag(1)−C(11) angle of 174.33(4)° and Ag(1)−C(1) and Ag(1)−C(11) separations of 2.077(1) and 2.082(1) Å, respectively. The NHC ligands are arranged so that the pyridyl portions are on the same side of the molecule. The imidazole portions of the two ligands are nearly coplanar with a dihedral angle of only 7.43° between the planes formed by these two moieties. This arrangement makes the coordination environment around the Ag center fairly flat and allows for longer-range pairwise intermolecular Ag···Ag contacts of 3.65 Å. Similar face-to-face interactions were observed in the closely related $[Ag(im(CH_2py)_2)_2]BF_4$ complexes reported earlier.[7]

Table 1. X-ray Crystallographic Data for Complexes **1**−**5**

	1	**2**	**3**	**4**·0.5 EtOH	**5**
formula	$C_{20}H_{22}AgBF_4N_6$	$C_{40}H_{44}Au_2B_2F_8N_{12}$	$C_{20}H_{22}AgAuBF_4N_6$	$C_{21}H_{22}Au_2B_2F_8N_6O_{0.5}$	$C_{34}H_{39}Ag_3B_3F_{12}N_{11}$
fw	541.12	1260.43	824.89	934.00	1185.80
cryst syst	monoclinic	monoclinic	orthorhombic	monoclinic	monoclinic
space group	$P2_1/n$	$P2_1/n$	*Pnma*	*C*2/*c*	*Cc*
a (Å)	13.7770(3)	11.0992(6)	15.5514(6)	21.2362(6)	11.0251(8)
b (Å)	11.3666(3)	20.236(1)	13.2092(5)	12.1942(3)	21.066(1)
c (Å)	14.7380(3)	19.301(1)	12.3050(5)	21.2244(6)	18.620(1)
β (deg)	110.57(1)	92.251(1)		109.890(1)	93.831(2)
V (Å^3)	2160.80(9)	4331.8(4)	2527.71(17)	5168.4(2)	4315.0(5)
Z	4	4	4	8	4
temp (K)	100(2)	100(2)	100(2)	100(2)	100(2)
R_1	0.0227	0.0363	0.0288	0.0661	0.0366
R_2 ($I > 2\sigma(I)$)	0.0591	0.0826	0.0695	0.1679	0.0531

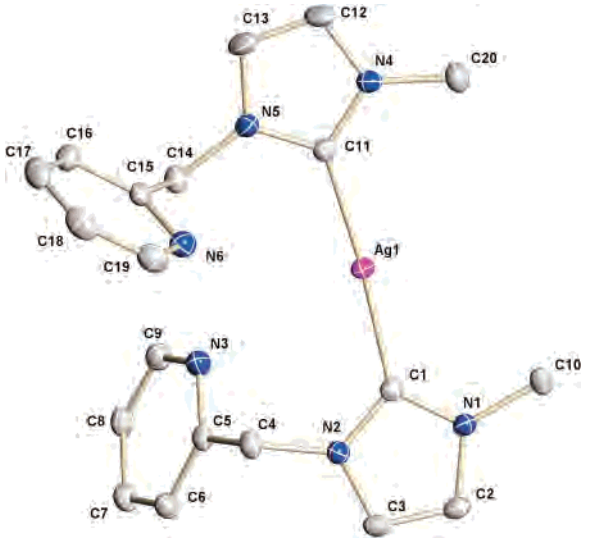

Figure 2. X-ray structural drawing of the cationic portion of [Ag(CH_3-im(CH_2py))$_2$]BF_4 (**1**) with 50% thermal ellipsoids. The hydrogen atoms were omitted for clarity.

Table 2. Selected Bond Distances (Å) and Angles (deg) for Complexes **1** and **2**

	1 (M = Ag)	**2** (M = Au)
M(1)−C(1)	2.077(1)	2.009(5)
M(1)−C(11)	2.082(1)	2.017(5)
C(1)−N(1)	1.3526(14)	1.366(6)
C(1)−N(2)	1.3555(14)	1.345(6)
N(1)−C(2)	1.3814(14)	1.387(7)
N(2)−C(3)	1.3846(15)	1.389(6)
C(2)−C(3)	1.3568(17)	1.344(8)
M···M	3.65	3.539
C(1)−M(1)−C(11)	174.33(4)	176.0(2)
N(2)−C(4)−C(5)	112.19(9)	112.1(4)
N(5)−C(14)−C(15)	111.17(10)	113.5(4)
N(1)−C(1)−N(2)	104.47(9)	104.6(4)
N(4)−C(11)−N(5)	104.37(10)	104.9(4)

The monometallic gold complex, [Au(CH_3im(CH_2py))$_2$]-BF_4 (**2**), is very similar, except that the asymmetric unit contains two cations arranged in a face-to-face fashion and two tetrafluoroborate anions. Selected bond distances and angles for the Au(1) containing cation are provided in Table 2. As can be seen in Figure 3, the geometry about each Au(I) center is nearly linear and two coordinate with C(1)−Au(1)−C(11) and C(21)−Au(1)−C(31) angles of 176.0(2) and 176.8(2)°, respectively. The Au−$C_{carbene}$ bond distances in **2** are slightly shorter than those measured in **1** with Au(1)−C(1), Au(1)−C(11), Au(2)−C(21), and Au(2)−C(31) distances of 2.009(5), 2.017(5), 2.017(4), and 2.019(5) Å respectively. In **2**, the picolyl arm of the NHC ligands are splayed back allowing for an intermolecular Au···Au separation of 3.539 Å. The imidazole rings maintain their nearly coplanar arrangement with dihedral angles of 8.23 and 10.83° between the planes formed by the imidazole rings on each gold center.

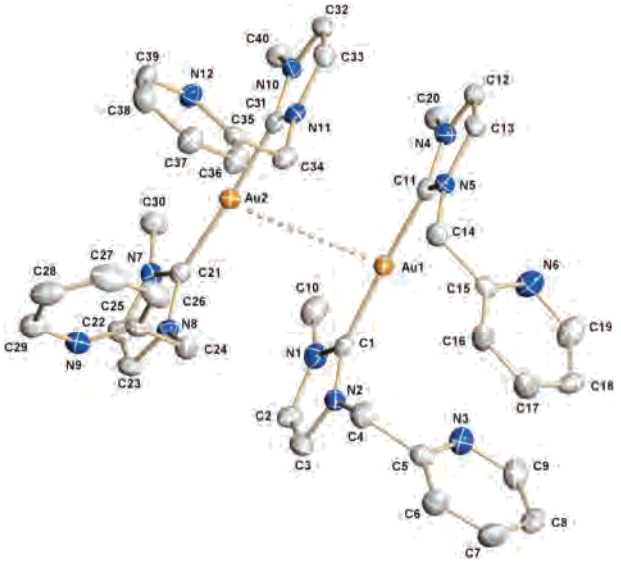

Figure 3. Thermal ellipsoid plot (50%) of [Au(CH_3im(CH_2py))$_2$]BF_4 (**2**) emphasizing the face-to-face interaction (3.539 Å) of the two cations in the asymmetric unit. The hydrogen atoms were omitted for clarity.

The addition of $AgBF_4$ to **2** ties up the uncoordinated pyridyl groups to produce the mixed-metal species [AuAg-(CH_3im(CH_2py))$_2$](BF_4)$_2$ (**3**). Complex **3** crystallizes in the orthorhombic space group *Pnma* with the asymmetric unit containing one-half of the cation and one tetrafluoroborate anion. As shown in Figure 4, the Au(1) and Ag(1) centers straddle a crystallographic mirror plane whose symmetry operation generates the remainder of the cation. The ligands are arranged in a head-to-head fashion and slightly hinged at the methylene linkages to accommodate the shortened Au(1)−Ag(1) separation of 3.0318(5) Å. This puckering distorts the C(1)−Au(1)−C(1A) and N(3)−Ag(1)−N(3A) angles from the ideal trans-spanning angle of 180° to 170.6-(2) and 154.6(2)°, respectively. Likewise, the Au(1)−C(1) separation at 2.030(4) Å is slightly longer than the corresponding separation in **2**. The Ag(1)−N(3) separation measures 2.167(3) Å, and an additional long-range contact

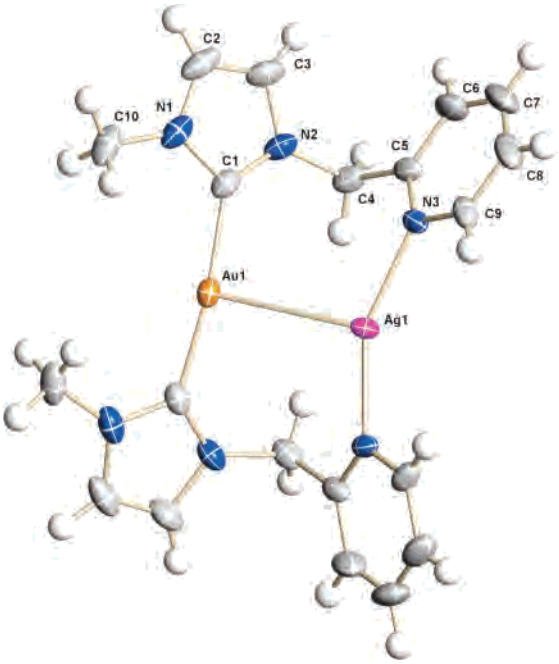

Figure 4. Crystal-structure drawing (thermal ellipsoid 50%) of the cationic portion of $[AuAg(CH_3im(CH_2py))_2](BF_4)_2$ (**3**). Only the asymmetric portion is numbered.

Table 3. Selected Bond Distances (Å) and Angles (deg) for Complex **3**

Au(1)−Ag(1)	3.0318(5)	C(1)−Au(1)−C(1A)	170.6(2)
Au(1)−C(1)	2.030(4)	N(3)−Ag(1)−N(3A)	154.58(16)
Ag(1)−N(3)	2.167(3)	C(1)−Au(1)−Ag(1)	94.28(10)
C(1)−N(1)	1.349(5)	N(3)−Ag(1)−Au(1)	102.56(8)
C(1)−N(2)	1.353(5)	N(2)−C(4)−C(5)	110.5(3)
N(1)−C(2)	1.386(7)	N(1)−C(1)−N(2)	104.7(4)
N(2)−C(3)	1.379(5)	C(1)−N(1)−C(2)	110.5(4)
C(2)−C(3)	1.339(7)	C(1)−N(2)−C(3)	111.1(4)
N(2)−C(4)	1.462(5)	C(2)−C(3)−N(2)	106.5(4)
C(4)−C(5)	1.504(6)	C(1)−Au(1)−Ag(1)−N(3)	0.02(13)

(2.833 Å) is found between Ag(1) and F(1) from the tetrafluoroborate anion. The methylene groups reside on the same face of the cation generating a pseudo-boat configuration for the twelve-membered ring. The N(2)−C(4)−C(5) angle at 110.5(3)° is close to the ideal tetrahedral angle, suggesting that there is little strain at this hingepoint. Additional bond distances and angles are presented in Table 3.

Isoelectronic $[Au_2(CH_3im(CH_2py))_2](BF_4)_2$ (**4**) crystallizes in the monoclinic space group *C*2/*c* with one cation, two tetrafluoroborate anions, and one-half of a disordered ethanol solvate. A view of the cation is presented in Figure 5, while selected bond distances and angles are given in Table 4. Unlike complex **3**, the NHC ligands in **4** are arranged in a head-to-tail fashion so that each gold atom is coordinated to one carbene and one pyridyl group in a nearly linear manner with C(1)−Au(1)−N(6) and C(11)−Au(2)−N(3) bond angles of 179.4(3) and 178.5(3)°, respectively. These gold centers are slightly twisted with respect to each other by approximately 60° as evidenced by the C(1)−Au(1)−Au(2)−C(11) and N(6)−Au(1)−Au(2)−N(3) torsion angles of 120.0(4) and 121.8(3)°, respectively. Further, at each gold center the pyridyl and NHC moieties are nearly orthogonal to each other with the angles between their respective planes

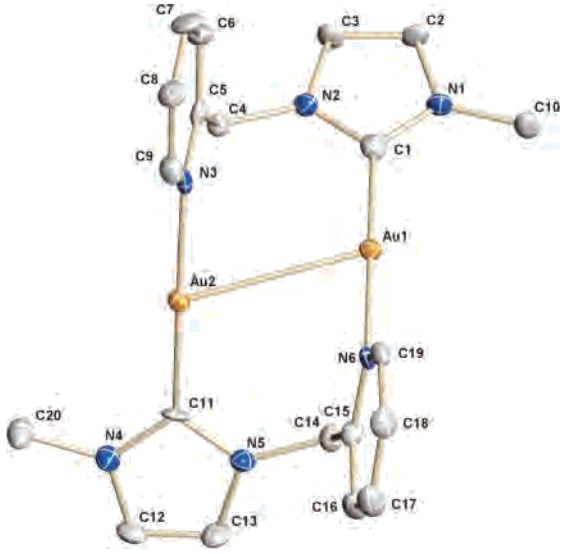

Figure 5. Thermal ellipsoid plot (50%) of $[Au_2(CH_3im(CH_2py))_2](BF_4)_2$ (**4**). The hydrogen atoms were omitted for clarity.

Table 4. Selected Bond Distances (Å) and Angles (deg) for Complex **4**

Au(1)−Au(2)	3.1730(5)	C(1)−Au(1)−N(6)	179.4(3)
Au(1)−C(1)	1.991(9)	C(11)−Au(2)−N(3)	178.5(3)
Au(1)−N(6)	2.087(8)	N(2)−C(4)−C(5)	110.4(7)
Au(2)−C(11)	2.000(8)	N(5)−C(14)−C(15)	110.6(7)
Au(2)−N(3)	2.081(8)	N(1)−C(1)−N(2)	105.1(8)
C(1)−N(1)	1.339(11)	N(4)−C(11)−N(5)	106.4(7)
C(1)−N(2)	1.358(11)	C(1)−Au(1)−Au(2)−N(3)	58.8(3)
C(11)−N(4)	1.340(11)	C(1)−Au(1)−Au(2)−C(11)	120.0(4)
C(11)−N(5)	1.351(11)	N(3)−Au(2)−Au(1)−N(6)	121.8(3)
		C(11)−Au(2)−Au(1)−N(6)	59.4(4)

of 78.73° for groups coordinated to Au(1) and 79.58 ° for those coordinated to Au(2). Within each ligand, the angles between the pyridyl and imidazole planes measure 85.21 and 83.12° for the ligands containing C(1) and C(11), respectively. The methylene hingepoints are relatively unstrained with N(2)−C(4)−C(5) and N(5)−C(14)−C(15) angles of 110.4(7) and 110.6(7)°, respectively. The Au(1)−Au(2) separation in **4** at 3.1730(5) Å is longer than the metal−metal separation measured in **3**, while the Au−C separations at 1.991(9) and 2.000(8) Å for Au(1)−C(1) and Au(2)−C(11), respectively, are slightly shorter. The Au−N bond distances are slightly longer with Au(1)−N(6) and Au(2)−N(3) distances of 2.087(8) and 2.081(8) Å, respectively.

Crystals of trimetallic $[Ag_3(CH_3im(CH_2py))_3(NCCH_3)_2](BF_4)_3$ (**5**) are reproducibly isolated from acetonitrile solutions of **5** by the slow addition of diethyl ether. As shown in Figure 6, the cation contains a nearly equilateral triangular Ag_3 core [Ag(1)−Ag(2)−Ag(3) = 60.36(2)°, Ag(1)−Ag(3)−Ag(2) = 60.12(1)°, and Ag(2)−Ag(1)−Ag(3) = 59.52(2)°] with exceptionally short Ag−Ag separations [Ag(1)−Ag(2) = 2.7765(8) Å, Ag(1)−Ag(3) = 2.7832(8) Å, and Ag(3)−Ag(2) = 2.7598(8) Å]. This core is buttressed by three bridging carbene ligands and three pyridyl groups, each oriented to one side of the Ag_3 trimetallic core. The carbene portions of two of the NHC ligands nearly symmetrically bridge their respective Ag−Ag linkages with C(11)−Ag(2), C(11)−Ag(3), C(21)−Ag(1), and C(21)−Ag(3) separations of 2.310(8), 2.184(7), 2.229(7), and 2.205(8) Å, respectively. The third NHC ligand, however, could

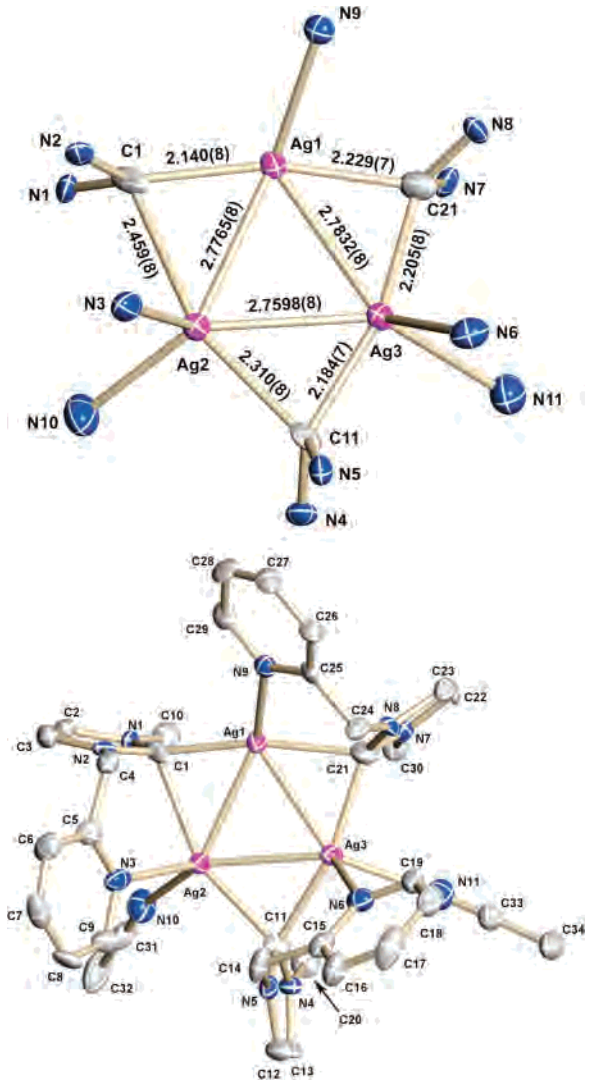

Figure 6. X-ray structural drawing emphasizing the core of **5** (top) and the complete cation (bottom) with 50% thermal ellipsoids. The hydrogen atoms were omitted.

Table 5. Selected Bond Distances (Å) and Angles (deg) for Complex **5**

Ag(1)−Ag(2)	2.7765(8)	Ag(1)−Ag(2)−Ag(3)	60.36(2)
Ag(1)−Ag(3)	2.7832(8)	Ag(1)−Ag(3)−Ag(2)	60.12(2)
Ag(2)−Ag(3)	2.7598(8)	Ag(2)−Ag(1)−Ag(3)	59.52(2)
C(1)−Ag(1)	2.140(8)	Ag(1)−C(1)−Ag(2)	73.9(3)
C(1)−Ag(2)	2.459(8)	Ag(2)−C(11)−Ag(3)	75.7(2)
C(11)−Ag(2)	2.310(8)	Ag(1)−C(21)−Ag(3)	77.8(2)
C(11)−Ag(3)	2.184(7)	C(1)−Ag(1)−C(21)	164.2(3)
C(21)−Ag(1)	2.229(7)	C(1)−Ag(2)−C(11)	157.9(3)
C(21)−Ag(3)	2.205(8)	C(11)−Ag(3)−C(21)	163.9(3)
Ag(1)−N(9)	2.344(6)	C(1)−Ag(1)−Ag(2)	58.3(2)
Ag(2)−N(3)	2.378(7)	C(1)−Ag(2)−Ag(1)	47.8(2)
Ag(2)−N(10)	2.341(8)	C(11)−Ag(2)−Ag(3)	50.1(2)
Ag(3)−N(6)	2.439(7)	C(11)−Ag(3)−Ag(2)	54.2(2)
Ag(3)−N(11)	2.472(7)	C(21)−Ag(1)−Ag(3)	50.7(2)
C(1)−N(1)	1.376(10)	C(21)−Ag(3)−Ag(1)	51.5(2)
C(1)−N(2)	1.370(9)	N(2)−C(4)−C(5)	112.1(6)
C(11)−N(4)	1.368(9)	N(5)−C(14)−C(15)	114.4(7)
C(11)−N(5)	1.379(10)	N(8)−C(24)−C(25)	110.3(6)
C(21)−N(7)	1.351(9)	N(10)−Ag(2)−Ag(3)	133.2(2)
C(21)−N(8)	1.349(9)	N(11)−Ag(3)−Ag(2)	142.8(2)
		N(1)−C(1)−N(2)	102.8(7)
		N(4)−C(11)−N(5)	102.6(7)
		N(7)−C(21)−N(8)	104.1(6)

be considered semi-bridging with one short Ag−C separation [C(1)−Ag(1) = 2.140(8) Å] and one long separation [C(1)−Ag(2) = 2.459(8) Å]. This asymmetry is further exemplified by the large difference in the C(1)−Ag(1)−Ag(2) and C(1)−Ag(2)−Ag(1) angles of 58.3(2) and 47.8(2)°, respectively. The Ag−N separations for the pyridyl groups are longer than those observed in **3** with Ag(1)−N(9), Ag(2)−N(3), and Ag(3)−N(6) measuring 2.344(6), 2.378(7), and 2.439(7) Å, respectively. Additionally, Ag(2) and Ag(3) are further coordinated to acetonitrile molecules [Ag(2)−N(10) = 2.341(8) Å and Ag(3)−N(11) = 2.472(7) Å]. The remaining Ag(1) center is left without a coordinated solvent, presumably a consequence of the semi-bridging NHC ligand which binds more strongly to this center than the coordinated pyridyl group. Attempts to add a third acetonitrile failed, and redissolving this material in acetonitrile followed by precipitation with diethyl ether produced identical crystals with identical ligation.

All of the complexes reported here are colorless with fairly featureless absorption bands deep in the UV. In acetonitrile, the carbene precursor, $[HCH_3im(CH_2py)]BF_4$, has an absorption band centered at ~260 nm with shoulders at 253 and 265 nm. Likewise, the absorption spectrum for the monosilver complex, **1**, is nearly identical except that these bands are less well-defined. In $[Au(CH_3im(CH_2py))_2]BF_4$ (**2**), these bands move only slightly with three peaks of nearly equal intensity distinguishable at 235, 246, and 261 nm. The mixed-metal dimer, $[AuAg(CH_3im(CH_2py))_2](BF_4)_2$ (**3**), shows two main bands at 245 and 261 nm along with two shoulders at 233 and 267 nm. These bands are also evident in the closely related digold species, $[Au_2(CH_3im(CH_2py))_2](BF_4)_2$ (**4**), but are significantly less resolved with one main band evident at 248 nm, along with a slightly less intense band at 232 nm and a faint shoulder at 267 nm. Last, the spectra of the acetonitrile solutions of $[Ag_3(CH_3im(CH_2py))_3(NCCH_3)_2](BF_4)_3$ (**5**) are similar to those of **1** with a poorly resolved absorption at 254 nm and a shoulder at 268 nm.

All of these complexes, including the carbene precursor, $[HCH_3im(CH_2py)]BF_4$, are intensely photoluminescent in the solid state and at low temperature (77 K) in a frozen solution and are moderately emissive in acetonitrile solution at room temperature. Specifically, the carbene precursor, $[HCH_3im(CH_2py)]BF_4$ (CH_3CN, 25 °C), exhibits a broad emission centered at ~440 nm (λ_{exi} = 300 nm). A nearly identical spectrum is observed upon freezing the solution at 77 K. The monometallic silver complex, **1**, exhibits an intense emission band at 460 nm (λ_{exi} = 370 nm), while under similar conditions, a slightly broader band is observed at 468 nm for the corresponding Au-containing solid, **2** (Supporting Information). At 77 K, these bands sharpen and intensify.

As shown in Figure 7, the emission spectra of the dimetallic complexes, **3** and **4**, are more interesting. At room temperature in acetonitrile, the mixed-metal complex, $[AuAg(CH_3im(CH_2py))_2](BF_4)_2$ (**3**), displays a sharp band at 416 nm similar to that of the free ligand while the homometallic dimer, $[Au_2(CH_3im(CH_2py))_2](BF_4)_2$ (**4**), has a significantly broader band centered at 475 nm. Freezing the solution at 77 K intensifies the signal for **3,** without changing the emission maxima, and likewise, the 475 nm signal for **4** intensifies, and a new band is produced at 423 nm, suggesting

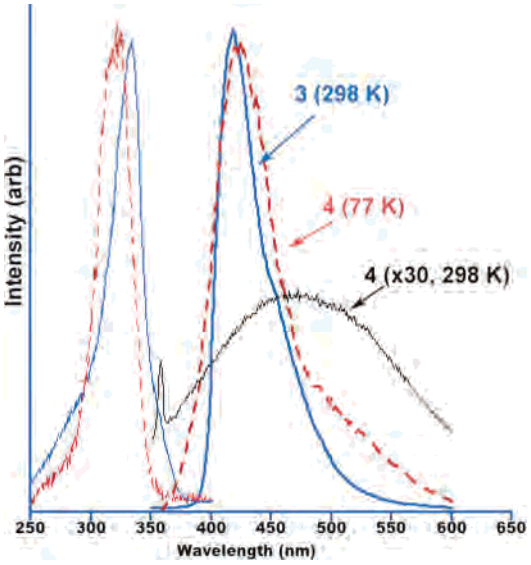

Figure 7. Emission (right) and excitation (left) spectra of **3** (blue traces) in acetonitrile at room temperature and **4** (red and black (x 30) traces) at room temperature and 77 K. The 77 K emission spectrum of **3** is nearly identical to its room-temperature spectrum and is not shown.

that more than one process is occurring. In the solid state (25 °C), the spectrum of **3** is unchanged from the solution state, but for **4** only the high-energy band is observed.

The solid-state emission spectrum of the trimetallic complex, $[Ag_3(CH_3im(CH_2py))_3(NCCH_3)_2](BF_4)_3$ (**5**), shows a very broad and intense emission band centered at 445 nm. At room temperature (CH_3CN), this band sharpens, loses intensity, and shifts slightly to 465 nm. Freezing this solution at 77 K causes this band to blue shift, and a sharp band is apparent at 401 nm.

Discussion

As illustrated here, the strong σ-donating ability[17,18] and relatively flat steric profile of the N-heterocyclic carbenes (NHC) make them ideal ligands[19] for stabilizing metal−metal interactions in solution and in the solid state. Complexes **1**−**5** are all easily prepared in good yield and are stable to moisture and air, but they are slightly photosensitive. Of these, the digold species (**4**) is the most photosensitive. All of these complexes are substitution inert except for **5** which appears to dissociate into a dimetallic in solution.

The formulation of a dimer in solution for **5** is supported both by the ^{1}H NMR spectroscopy, which shows a coupling pattern similar to that of the head-to-tail Au_2 dimer, and the mass spectrum, whose most intense peak and isotopomer pattern are consistent with the dimetallic formulation. Additionally, peaks corresponding to the mono- and bis-acetonitrile complexes are evident with only a very small peak observed for the trimetallic species. In the solid state, however, only $[Ag_3(CH_3im(CH_2py))_3(NCCH_3)_2]^{3+}$ is observed even after repeated crystallizations. Attempts to add a third acetonitrile molecule failed, and only complex **5** was recovered.

The origin of the asymmetrical ligation is unknown but must be related to the observation of a semi-bridging carbene in the solid-state structure of **5**. The strong σ donation of the C(1)-containing NHC ligand to Ag(1) limits the need for solvent ligation at this silver center. Further stabilization at Ag(1) is achieved by slightly contracting the coordinated pyridyl group toward Ag(1). Interestingly, the introduction of the semi-bridging carbene does not significantly alter the metal−metal bonding in **5**. In fact, the Ag−Ag separations observed in **5** are nearly identical to those [2.7718(9), 2.7688(9), and 2.7249(10) Å] found in the closely related $[Ag_3((pyCH_2)_2im)_3](BF_4)_3$ complex,[7] where each silver center is symmetrically bridged by an NHC ligand and equally coordinated to two pyridyl groups. However, unlike complex **5**, the $[Ag_3((pyCH_2)_2im)_3](BF_4)_3$ complex maintains it Ag_3 core in solution.

NHC ligands asymmetrically bound to Ag are rare but have been observed elsewhere. Youngs and co-workers[20] have extensively investigated NHC-linked cyclophane complexes and recently reported asymmetrically bound NHC ligands in tetranuclear Ag_4 clusters. Formulated as σ/π-bonding interactions, these carbenes have remarkably similar Ag−C separations ranging from 2.13 to 2.41 Å. Likewise, these tetranuclear complexes also contain relatively short Ag−Ag separations ranging from 2.7680(9) to 2.9712(11) Å. The Ag−Ag separations observed in complex **5** are also short and are likely to be a consequence of the excellent stabilizing ability of the bridging NHC ligands. Triangular Ag_3 cores are not particularly uncommon in the literature, and a fairly large range of Ag−Ag interactions are observed with the shortest belonging to those that also have anionic ligands capping the trigonal face or bridging the Ag−Ag bond. For example, in the well-studied phosphine-bridged $[Ag_3(PPh_2CH_2PPh_2)_3]^{3+}$ complexes which usually contain anionic auxiliary ligands coordinated to the triangular face,[21,22,23] the Ag−Ag separations are much longer ranging from ∼3.0 to 3.4 Å.

The difference in fluxional behavior between **3** and **4** likely originates from the opposing ligand arrangements in these complexes. In the mixed-metal $[AuAg(CH_3im(CH_2py))_2](BF_4)_2$ (**3**) complex, the soft donor groups of the carbene portion of the $CH_3im(CH_2py)$ ligands remain coordinated to the Au(I) atom, while the pyridyl groups prefer the harder Ag(I) center consistent with other P−N donor ligands. This head-to-head arrangement generates a twelve-membered pseudo-boat configuration which is very fluxional at room temperature, as evidenced by the relatively small barrier measured in the VT-^{1}H NMR for the interconversion of the methylene protons. Conversely, in the absence of a mutually favorable hard/soft interaction, the two $CH_3im(CH_2py)$ ligands adopt a more symmetrical head-to-tail arrangement

(17) Lee, M.-T.; Hu, C.-H. *Organometallics* **2004**, *23*, 976.
(18) Hu, X.; Castro-Rodriguez, I.; Olsen, K.; Meyer, K. *Organometallics* **2004**, *23*, 755.
(19) Herrmann, W. A. *Angew. Chem., Int. Ed.* **2002**, *41*, 1290.
(20) Garrison, J. C.; Simons, R. S.; Kofron, W. G.; Tessier, C. A.; Youngs, W. J. *Chem. Commun.* **2001**, 1780. (b) Garrison, J. C.; Simons, R. S.; Tessier, C. A.; Youngs, W. J. *J. Organomet. Chem.* **2003**, *673*, 1.
(21) Yam, V. W.-W.; Fung, W. K.-M.; Cheung, K.-K. *Organometallics* **1997**, *16*, 2032.
(22) Yam, V. W.-W.; Fung, W. K.-M.; Cheung, K. K. *Chem. Commun.* **1997**, 963
(23) Zhou, W.-B.; Dong, Z.-C.; Song, J.-L.; Zeng, H.-Y.; Cao, R.; Guo, G.-C.; Huang, J.-S.; Li, J. *J. Cluster Sci.* **2002**, *13*, 119.

in the homodimetallic $[Au_2(CH_3im(CH_2py))_2](BF_4)_2$ complex (**4**). Here, the im-Au-py vectors are twisted by about 60° with respect to each other, and it is hypothesized that this twisting motion, rather than a boat−chair isomerization, leads to the slightly higher barrier observed for the interconversion of the methylene signals in **4**. As shown in Figure 5, the pyridyl and NHC groups coordinated to each gold center are nearly orthogonal to each other, which might suggest an optimization of the π-back-bonding. However, recent calculations[24] suggest that, although the Ag−NHC π-back-bonding measurably contributes to the M−L bond strength, the rotational barrier between the coplanar and perpendicular coordination modes is negligible and these groups could easily twist to accommodate the complexes fluxional behavior.

The Au−Ag separation of 3.0318(5) Å, in **3**, and the Au−Au separation of 3.1730(5) Å, in **4**, are consistent with other Ag and Au phosphine and phosphinopyridine complexes. For example, Schmidbaur and co-workers reported a 2.820 Å Au−Ag separation in the $[AuAg(Ph_2Ppy)_2]^{2+}$ complex[25] and a shorter Au−Au separation of 2.776 Å in the $[Au_2(Ph_2Ppy)_2]^{2+}$ homolog.[26] Likewise, using the 2-diphenylphosphino-1-methylimidazole (dpim) ligand, we observed a ∼2.82 Å Au−Au separation in $[Au_2(dpim)_2]^{2+}$ and a ∼2.86 Å Au−Ag separation in the three-coordinate $[AuAg(dpim)_3]^{2+}$ dimer.[27] Laguna, Eisenberg, and co-workers[28] found slightly longer Au−Ag distances ranging from 2.8985(5) to 2.9690(5) Å in their chalcogen-capped $Au_3Ag(Ph_2P)_3$ cluster. Longer separations of 3.058(1) Å for $[Ag_2(dppm)_2]^{2+}$,[29] 2.982 Å for $[Au_2(dppm)_2]^{2+}$,[30] and 2.9063(9)−3.0132(6) Å for various salts of $[Au_2(dcpm)_2]^{2+}$[31] are observed when the more flexible phosphine backbones are employed [dppm is bis(diphenylphosphino)methane and dcpm is bis(dicyclohexylphosphino)methane].

While reports of photoluminescent Ag(I)− and Au(I)−NHC complexes are still relatively scarce,[32,33,34,35] an impressive amount of literature on the photophysical properties of the closely related phosphine or bridged d^{10} complexes exists.[36,37,38] The nature of the excited states in these complexes is equally vast and includes intraligand (IL) states, metal-centered (MC) states, and depending on the ligand systems, various charge-transfer states. All of the complexes reported here, including the ligand precursor, are photoluminescent in solution and in the solid state. The assignment of the excited state for the complexes reported here is beyond the scope of this work, especially, since the dimetallic complexes, **3** and **4** also contain weak $d^{10}-d^{10}$ interactions, which significantly complicate an assignment. Regardless of the origin of the emission process, the intense luminescent properties of these materials make them attractive targets for luminescent applications including OLEDs[39] and further photophysical study.

In this work, we have further demonstrated the utility of NHC ligands as supports for generating metal−metal interactions. These ligands are exceptionally easy to synthesize, form very strong metal−ligand bonds, and their flat steric profile allows for close metal−metal interactions. These properties suggest that substituted NHC ligands will be ideal candidates to build other $d^{10}-d^{10}$, $d^{10}-d^{8}$, and $d^{8}-d^{8}$ systems.

Acknowledgment. This work and the X-ray diffractometer purchase were supported by the National Science Foundation (CHE-0091180 and CHE-0226402).

Supporting Information Available: Crystallographic data in CIF format for complexes 1−**5**, VT-NMR spectroscopy for complexes **3** and **4**, and emission spectra for complexes **1** and **2**. This material is available free of charge via the Internet at http://pubs.acs.org.

IC050604+

(24) Nemcsok, D.; Wichmann, K.; Frenking, G. *Organometallics* **2004**, *23*, 3640.
(25) Olmos, M. E.; Schier, A.; Schmidbaur, H. *Z. Naturforsch., B* **1997**, *52*, 203.
(26) Inoguchi, Y.; Milewski-Mahrla, B.; Schmidbaur, H. *Chem. Ber.* **1982**, *115*, 3085.
(27) Catalano, V. J.; Horner, S. J. *Inorg. Chem.* **2003**, *42*, 8430.
(28) Wang, Q.-M.; Lee, Y.-A.; Crespo, O.; Deaton, J.; Tang, C.; Gysling, H. J.; Gimeno, M. C.; Larraz, C.; Villacampa, M. D.; Laguna, A.; Eisenberg, R. *J. Am. Chem. Soc.* **2004**, *126*, 9488.
(29) Wei, Q.; Yin, G.; Chen, Z. *Acta Crystallogr., Sect. E* **2003**, *59*, 232.
(30) King, C.; Wang, J.-C.; Khan, M. N. I.; Fackler, J. P., Jr. *Inorg. Chem.* **1989**, *28*, 2145.
(31) Fu, W.-F.; Chan, K.-C.; Miskowski, V.-M.; Che, C.-M. *Angew. Chem., Int. Ed.* **1999**, *38*, 2783. (b) Leung, K. H.; Phillips, D. L.; Mao, Z.; Che, C.-M.; Miskowski, V. M.; Chan, C.-K. *Inorg. Chem.* **2002**, *41*, 2054. (c) Leung, K. H.; Phillips, D. L.; Tse, M.-C.; Che, C.-M.; Miskowski, V. M. *J. Am. Chem. Soc.* **1999**, *121*, 4799.
(32) Wang, H. M. J.; Vasam, C. S.; Tsai, T. Y. R.; Chen, S.-H.; Chang, A. H. H.; Lin, I. J. B. *Organometallics* **2005**, *24*, 486.
(33) Wang, H. M. J.; Chen, C. Y. L.; Lin, I. J. B. *Organometallics* **1999**, *18*, 1216.
(34) Lee, K. M.; Wang, H. M. J.; Lin, I. J. B. *J. Chem. Soc., Dalton Trans.* **2002**, 2852.
(35) Liu, Q. X.; Xu, F. B.; Li, Q. S.; Zeng, X. S.; Leng, X. B.; Chou, Y. L.; Zhang, Z. Z. *Organometallics* **2003**, *22*, 309.
(36) Forward, J. M.; Fackler, J. P., Jr.; Assefa, Z. In *Optoelectronic Properties of Inorganic Compounds*; Roundhill, D. M., Fackler, J. P., Jr., Eds.; Plenum Press: New York, 1999; p 195.
(37) Yam, V. W.-W.; Lo, K. K.-W. *Chem. Soc. Rev.* **1999**, *28*, 323.
(38) Harvey, P. D. *Macromol. Symp.* **2004**, *209*, 81.
(39) Yersin, H. *Topics Curr. Chem.* **2004**, *241*, 1.